의학박사 학위논문

Effect of Hyaluronic Acid-Hydroxyapatite Filler on Collagen and Elastic Fiber Regeneration in a Nude Mouse Model

누드마우스 모델에서 hyaluronic acid−hydroxyapatite 복합 필러의 피부 콜라겐 및 탄성섬유 재생효과

2016 년 08 월

서울대학교 대학원
의학과 성형외과학 전공
범 영 방

누드마우스 모델에서 hyaluronic acid-hydroxyapatite 복합 필러의 피부 콜라겐 및 탄성섬유 재생효과

지도교수 김 석 화

이 논문을 의학박사 학위논문으로 제출함

2016 년 04 월

서울대학교 대학원

의학과 성형외과학 전공

범 영 방

범영방의 의학박사 학위논문을 인준함

2016 년 06 월

위 원 장 (인)

부위원장 (인)

위 원 (인)

위 원 (인)

위 원 (인)

Effect of Hyaluronic Acid-Hydroxyapatite Filler on Collagen and Elastic Fiber Regeneration in a Nude Mouse Model

by

Ying Fang Fan

A thesis submitted to the Department of Plastic and Reconstructive Surgery in partial fulfillment of the requirements for the Degree of Doctor of Philosophy in Medicine at Seoul National University College of Medicine

June 2016

Approved by Thesis Committee:

Professor _____ **Chairman**

Professor _____ **Vice chairman**

Professor _____

Professor _____

Professor _____

ABSTRACT

Effect of Hyaluronic Acid-Hydroxyapatite Filler on Collagen and Elastic Fiber Regeneration in a Nude Mouse Model

Yingfang Fan

College of Medicine

Department of Plastic and Reconstructive Surgery

The Graduate School

Seoul National Unversity

Introduction: Compared to pure hyaluronic acid filler, cross-linked hyaluronic acid (HAc) filler has superior biocompatibility and longevity as long-lasting effective dermal fillers. Herein, we investigated effects and longevity of HAc-hydroxyapatite (HAp) filler on collagen and elastic fiber regeneration in a nude mouse model.

Methods: Six-week-old female BALB/c-nude mice were classified into 5 groups: normal skin, Radiesse, Restylane, HAc-nanoHAp, and HAc-microHAp. Fillers (200 μl) were injected to evenly fill the backs of mice. Filler volume was compared by MRI after 0, 1, 4, 8, and 12 weeks. Skin biopsies were performed to investigate collagen and elastic fiber synthesis after filler injections. Western blot analysis, real time-PCR, and immunohistochemistry were used to investigate protein and gene expression changes. Organ (liver, lung, spleen, and kidney) toxicity of HAc-nanoHAp was determined by hematoxylin & eosin staining after 12 weeks.

Results: Results of these analyses suggest that HAc-nanoHAp and HAc-microHAp hydrogels had good longevity and promoted collagen and elastic fiber formation via the TGF-ß pathway.

Conclusion: HAc-HAp filler could play an important role in collagen and elastic fiber regeneration. Further research should focus on the role of hyaluronic acid and hydroxyapatite composite fillers in photoaging in animal models and effects on skin, including on elasticity and tension strength.

Keywords: Elastic fiber, Collagen, Hyaluronic acid, Hydroxyapatite, Hyaluronic acid-hydroxyapatite, Filler

Student Number: 2014-30869

CONTENTS

LIST OF TABLES AND FIGURES

LIST OF ABBREVIATION

BDDE, Butanediol diglycidyl ether

CaP, Calcium phosphate

CMC, Carboxymethylcellulose

DAB, Diaminobenzidine

EDTA, Ethylenediaminetetraacetic acid

EGFR, Epidermal growth factor receptor

ERK, Extracellular signal-regulated kinase

HAc, Hyaluronic acid

HAp, Hydroxyapatite

H&E, Hematoxylin and eosin

MAPK, Mitogen-activated protein kinase

PCR, Polymerase chain reaction

PVDF, Polyvinylidene difluoride

TGF-ß, Transforming growth factor beta

INTRODUCTION

As the standard of living rises, people pay more attention to physical beauty. A series of pharmaceuticals, cosmetic agents, and medical devices have been developed to effectively resist skin aging (1). Skin aging is associated with dermal matrix alterations and atrophy (2). Decreases in collagen and elastic fibers in the extracellular matrix can cause skin aging and skin laxity (3). To improve skin defects, dermal fillers have advanced greatly in the past decade in the field of esthetic medicine (2-5).

The most commonly used material for dermal filler is hyaluronic acid (HAc) (6). HAc filler exhibits superior bioactivity and biocompatibility properties compared with other fillers along with natural degradation (7). Cross-linked HA filler stimulates fibroblast cells to produce collagen fiber via the TGF-ß/Smad pathway (1, 3, 8). However, the precise pathway is not clear. In the dermal microenvironment, collagen stimulation is associated with the upregulation of type II TGF-β receptor, which is the major regulator of type I procollagen synthesis in human skin (8-10). HAc facilitates TGF-ß1-dependent fibroblast proliferation by promoting the interaction between CD44 and Epidermal growth factor receptor (EGFR), which then promotes MAPK/ERK phosphorylation, inducing cell proliferation (11). We examined the mechanism of collagen formation after HAc filler injection. HAc can also promote the growth of elastic fibers (1, 3). Although the mechanism of HAc-induced elastic

fiber generation remains unclear, some studies have shown that TGF-ß stimulates the expression of many genes that are necessary for the production of elastic fibers, including elastin and fibrillin (12, 13). Despite their many advantages, HAc-based dermal fillers often last for only a few months *in vivo* owing to rapid enzymatic degradation (5).

Calcium phosphate (CaP)-based bioceramics can also be incorporated into bioactive and long-lasting fillers (14). Radiesse (calcium hydroxyapatite; CaHA, Merz Pharmaceuticals GmbH, Frankfurt, Germany) is a candidate filler material with excellent bioactivity and longevity (15). Owing to its CaHA microspheres, Radiesse increases collagen and elastic fibers, resulting in a local fibroblastic response after injection (16, 17). It also shows great longevity, lasting more than six months (18). However, carboxymethylcellulose (CMC), which represents 70% of Radiesse, is less able to promote cell affinity to induce collagen formation than HAc (6, 19). Composite fillers composed of both HAc and hydroxyapatite (HAp) have not been reported, because HAc, as the sole gel carrier instead of CMC, has limited physical and mechanical stability.

In this study, we developed two multifunctional composite hydrogel fillers based on both HAc and HAp to promote long-lasting skin extracellular matrix stimulation: HAc-nanoHAp fillers and HAc-microHAp fillers. In particular, we used *in situ* precipitation of nano-sized HAp particles with HAc chains to enhance mechanical stability against enzymatic degradation. In addition to the application of these

composite systems to dermal fillers, we systematically compared longevity *in vivo* by monitoring the volume change of fillers by MRI and determined the mechanisms underlying the biological responses to HAc and HAp.

MATERIALS AND METHODS

HAc-HAp composite filler preparation

HAc-nanoHAp composite hydrogel

HAc (10 w/v%) in 0.2 N NaOH solution was cross-linked via the cross-linker 1,4-butanediol diglycidyl ether (BDDE) for 12 h at 40℃. The cross-linked hydrogel was dialyzed and fully swollen in distilled water at room temperature. It was then immersed in a solution of $CaCl_2$ and H_3PO_4 for 2 h. Subsequently, it was dipped in 15% NH_4OH solution for 30 min to precipitate 30 wt% of nanoHAp within the hydrogel. The average size of nanoHAp particles was 200 nm.

HAc-microHAp composite hydrogel

Prior to crosslinking, HAp microspheres were prepared by spray-drying a solution consisting of HAp powder, PVB, and KD6, followed by heat treatment at 500℃ for 2 h and 1200℃ for 2 h. HAp microspheres (30 vol%) with an average size of 20 μm were homogeneously mixed into the HAc solution with BDDE crosslinker. The mixture was sealed and maintained at 40℃ for 12 h to allow gelation, followed by washing and swelling in PBS (refreshed daily) at room temperature.

Composite filler preparation

All composite hydrogels were homogenized at 7000 rpm for 5 min and autoclaved at 121℃ for 30 min to prepare the gel particles for injection through a needle.

Animal experiments

Twenty-nine 5-week-old female BALB/c nude mice were obtained from Orient Bio Inc. (Seongnam, Korea), and were fed a standard diet. After resting for 1 week, the mice were injected with Radiesse, Restylane, HAc-nanoHAp, and HAc-microHAp. The treatment groups were compared with uninjected mice. A 30-gauge needle was used to inject the filler between the panniculus adiposus layer and panniculus carnosus. Four injections were administered per mouse. For the initial injection, there were 24 animals per group. The results were compared at 1, 4, 8, and 12 weeks after the injection. At weeks 1, 4, and 8, three mice skin biopsies were collected for real-time PCR and western blot analyses, and two mice skin biopsy was collected for histological observations. At week 12, seven mouse skin biopsies were collected for real-time PCR and western blot analyses, and two mice skin biopsy was collected for histological observations. After four weeks, an additional five mice were injected. For the magnetic resonance image volumetric analysis, five mice were examined at weeks 0, 1, 4, 8, and 12. Finally, 29 mice per group were analyzed. This animal experiment was approved by the Institutional Animal Care and Use Committee of the Seoul National University (IACUC Protocol No. 15-0075).

Magnetic resonance image (MRI) volumetric analysis

At weeks 0, 1, 4, 8, and 12 all of the groups were examined by an MRI volumetric analysis under isoflurane/O_2 (1.5% isoflurane, 1.0 l/min O_2). The Agilent 9.4T/160AS (Agilent Technologies, Santa Clara, CA, USA) magnetic resonance scanner and the Millipede Coil (1-ch coil) (Agilent Technologies) were used. Both axial and coronal images were obtained. T2 maps were generated. The axial T2-weighted image slice thickness was 0.3 mm and the coronal T2-weighted image slice thickness was 1.0 mm. The axial T2-weighted image for the volumetric analysis was obtained using a SNUH PACS Viewer (Seoul National University, Seoul, Korea).

Histological observations

At weeks 1, 4, 8, and 12, the injected skin biopsies measuring 1 cm × 1 cm were extracted and were fixed in a 10% formaldehyde solution for 24 h, after which they were embedded in paraffin and sectioned at 6 μm. The sections were stained using hematoxylin and eosin (H&E), Masson's trichrome, and Verhoeff-Van Gieson, and were analyzed using image analysis software (ImageJ; National Institutes of Health, Bethesda, MD, USA) (Leica QWin V3; Leica Microsystems Cambridge, England, UK). To determine the organ (liver, lung, spleen, and kidney) toxicity of HAc-nanoHAp nanoparticles, H&E staining was performed after 12 weeks.

Immunohistochemical analysis

Tissue sections were cut and placed on microscope slides. The Discovery XT automated immunohistochemistry stainer (Ventana Medical Systems, Inc., Tucson, AZ, USA) was used to stain slides and the Ventana Chromo Map Kit (Ventana Medical Systems) was used for detection. The tissue sections were deparaffinized, and CC1 standard (buffer containing Tris, borate, and ethylenediaminetetraacetic acid (EDTA), pH 8.4) was used to retrieve the antigen. Inhibitor D (3% H_2O_2, endogenous peroxidase) was plugged in for 4 min at 37 ℃. The slides were incubated with anti-tropoelastin (Abcam, Cambridge, MA, USA) for 32 min at 37 ℃, and OmniMap anti-rabbit horseradish peroxidase as a secondary antibody for 20 min at 37 ℃. The other slides were incubated with vimentin (Abcam) for 32 min at 37 ℃, and with an OmniMap anti-rabbit horseradish peroxidase secondary antibody for 20 min at 37 ℃. The slides were incubated in diaminobenzidine (DAB) with H_2O_2 substrate for 8 min at 37 ℃ followed by hematoxylin bluing reagent counterstaining at 37 ℃. A Tris buffer at pH 7.6 was used as the washing solution. Each slide was measured at five locations, and mean values were compared. The stained slides were evaluated using image analysis software (Leica QWin V3 and Leica Microsystems CMS GmbH, Wetzlar, Germany).

Real-time polymerase chain reaction (PCR)

The fillers of injected skin biopsies were removed, and the remaining skin tissues (i.e.,

the epidermis, dermis, and panniculus adiposus layer) were frozen at -80℃. Ribonucleic acid (RNA) was isolated from frozen tissues (50 mg) using TRIzol reagent (500 ml) (Molecular Research Center, Cincinnati, OH, USA) and a homogenizer, resuspended in RNase-free water and quantified with a UV spectrophotometer. Single-strand complementary DNA (cDNA) was prepared from 1 mg of total RNA in a 20-ml reaction volume using a TOPscript™ RT DryMIX (Enzynomics, Daejeon, Korea) according to the manufacturer's instructions. Real-time polymerase chain reaction (PCR) was performed on an ABI 7500 machine with SYBR Premix Ex Taq™ (TaKaRa, Otsu, Japan). PCR conditions were as follows: 15-m hot start at 95 ℃, followed by 40 cycles of 10 s at 95 ℃, 15 s at 60 ℃ and 30 s at 72℃. The average threshold cycle for each gene was determined from triplicate reactions. The gene expression levels were normalized to that of the ß-actin gene. The target genes were *EGFR*, *Smad2*, *Smad3*, procollagen, elastin, and fibrillin. Real-time PCR was performed three times for each mouse gene.

Western blot analysis

The fillers of injected skin biopsies were removed, and the remaining skin tissues (i.e., the epidermis, dermis, and subcutaneous fat) were frozen at -80℃. Frozen samples were homogenized in lysis buffer. The tissues lysates were centrifuged at 14,000 rpm for 10 min, and the supernatants were used to perform the western blot analysis. Protein concentration was quantified by a Bradford protein assay (Bio-Rad Laboratories, Hercules, CA, USA). All of the samples were mixed with Halt™

Protease and Phosphatase inhibitor Cocktail, EDTA-free (100X) (ThermoFisher Scientific, Waltham, MA, USA). Equal amounts of proteins were loaded onto a 10% sodium dodecyl sulfate polyacrylamide gel. The protein samples were transferred electrophoretically to polyvinylidene difluoride (PVDF) membranes. Then, the membranes were blocked with 5% skim milk in Tris-buffered saline (pH 7.4) and 0.1% Tween-20 for 1 h at room temperature. They were incubated with primary antibodies overnight at 4℃ and then with secondary antibodies for 1 h at room temperature. The primary antibodies were anti-mouse collagen type 1 (Abcam), anti-EGFR (Abcam), anti-TGFß (Abcam), anti-Smad2/3 (Cell Signaling Technology, Danvers, MA, USA), anti-MAPK (Erk1/2) (Cell Signaling Technology), anti-phosphorylated MAPK (Erk1/2) (Cell Signaling Technology), anti-Smad7 (Santa Cruz Biotechnology, Dallas, TX, USA) and anti-ß-Actin (Abcam) were used at dilutions of 1:500 to 1:30000. The second antibody was anti-rabbit IgG (Abcam). Proteins were visualized by enhanced chemiluminescence (Thermo Scientific, Rockford, IL, USA). The western blots were performed three times per mouse protein. The western blot data were quantified using a band-intensity densitometric analysis (ImageJ).

Statistical analysis

All data were analyzed using the Kruskal–Wallis test with IBM SPSS software version 20.0 (IBM Corporation, Armonk, NY, USA). Step-up Mann–Whitney tests were used with a multiple comparison adjustment. A *P*-value of less than 0.05 was considered statistically significant.

RESULTS

Imaging and MRI volumetric analyses

After 1, 4, 8, and 12 weeks, the remaining filler volume for all filler groups decreased, especially in the Restylane group (Figure 1a). The coronal T2-weighted image was obtained, with a slice thickness of 1.0 mm (Figure 1b). The axial T2-weighted image (slice thickness: 0.3 mm) was used for the volume analysis. Greater stability was observed for the HAc-nanoHAp group than the other 3 groups. After 4 weeks, the remaining filler was significantly greater in the HAc-nanoHAp group than the Restylane group, and was higher in the HAc-microHAp group than in the Radiesse group ($P < 0.05$). After 8 and 12 weeks, the remaining filler was significantly higher for the HAc-microHAp group and the HAc-nanoHAp group than the Restylane group ($P < 0.01$), and was significantly greater in the HAc-nanoHAp group than the Radiesse group (Figure 1c) ($P < 0.05$).

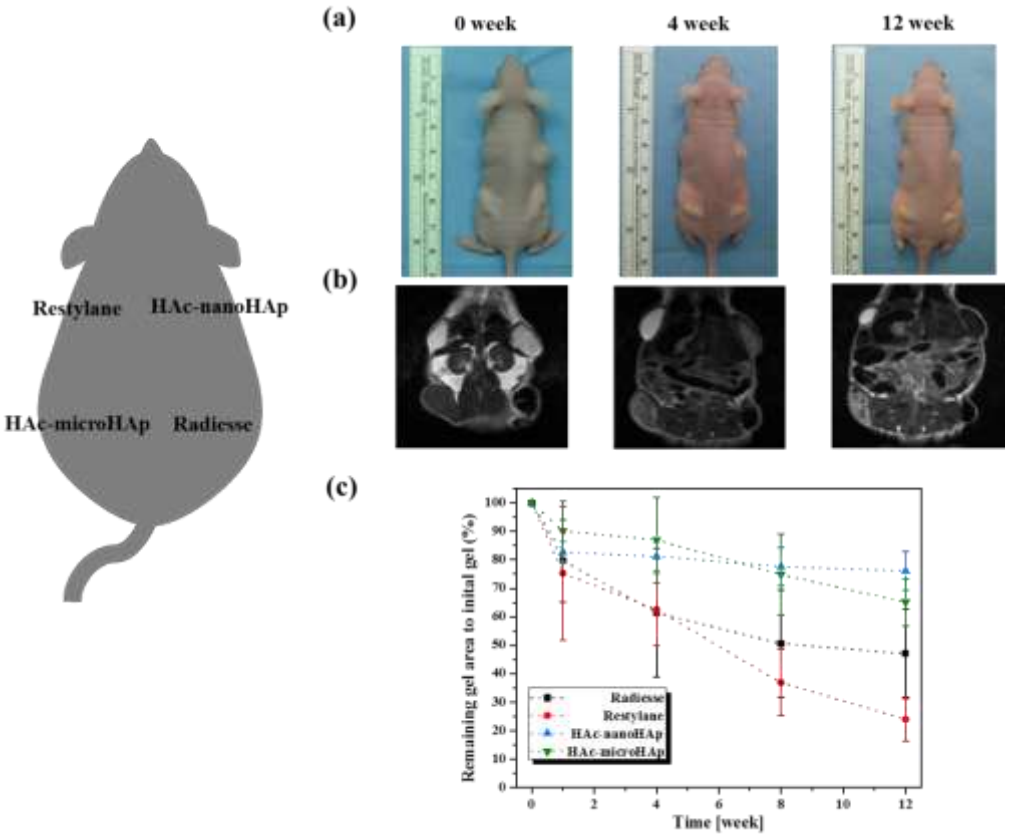

Figure 1. Photographs and results of MRI volumetric analysis.

Four injections were administered per mouse (the gray image). **(a**) Photographs of the skin surface and the corresponding filler volumes. Images show the filler groups at 0, 1, 4, 8, and 12 weeks after filler injection. For all groups, the filler volume decreased from week 0 to week 12, especially for the Restylane group. **(b)** The coronal T2-weighted image. Image slice thickness was 1.0 mm. **(c)** Volumetric analysis for the filler groups. The axial T2-weighted image (slice thickness: 0.3 mm) was used for the volumetric analysis. The stability of HAc-nanoHAp group was better than that of the

other 3 groups. After 4 weeks, the remaining filler was significantly greater in the HAc-nanoHAp group than the Restylane group, and was higher in the HAc-microHAp group than the Radiesse group (*$P < 0.05$). After 8 and 12 weeks, the remaining filler was significantly higher for the HAc-microHAp group and the HAc-nanoHAp group than the Restylane group (*$P < 0.01$); the remaining filler was significantly greater in the HAc-nanoHAp group than the Radiesse group (*$P < 0.05$).

Dermal thickness observations

Mouse skin samples were stained with H&E at weeks 1, 4, 8, and 12. Based on H&E staining, after 4 weeks, the dermises in skin samples were thicker than they were at week 1 (Figure 2a). All filler groups showed a consistent increase in dermal thickness with age. At week 1, the HAc-microHAp group was the first to exhibit an increase. At week 12, the HAc-HAp group had a significantly greater thickness than the Restylane group (Figure 2b) ($P < 0.01$).

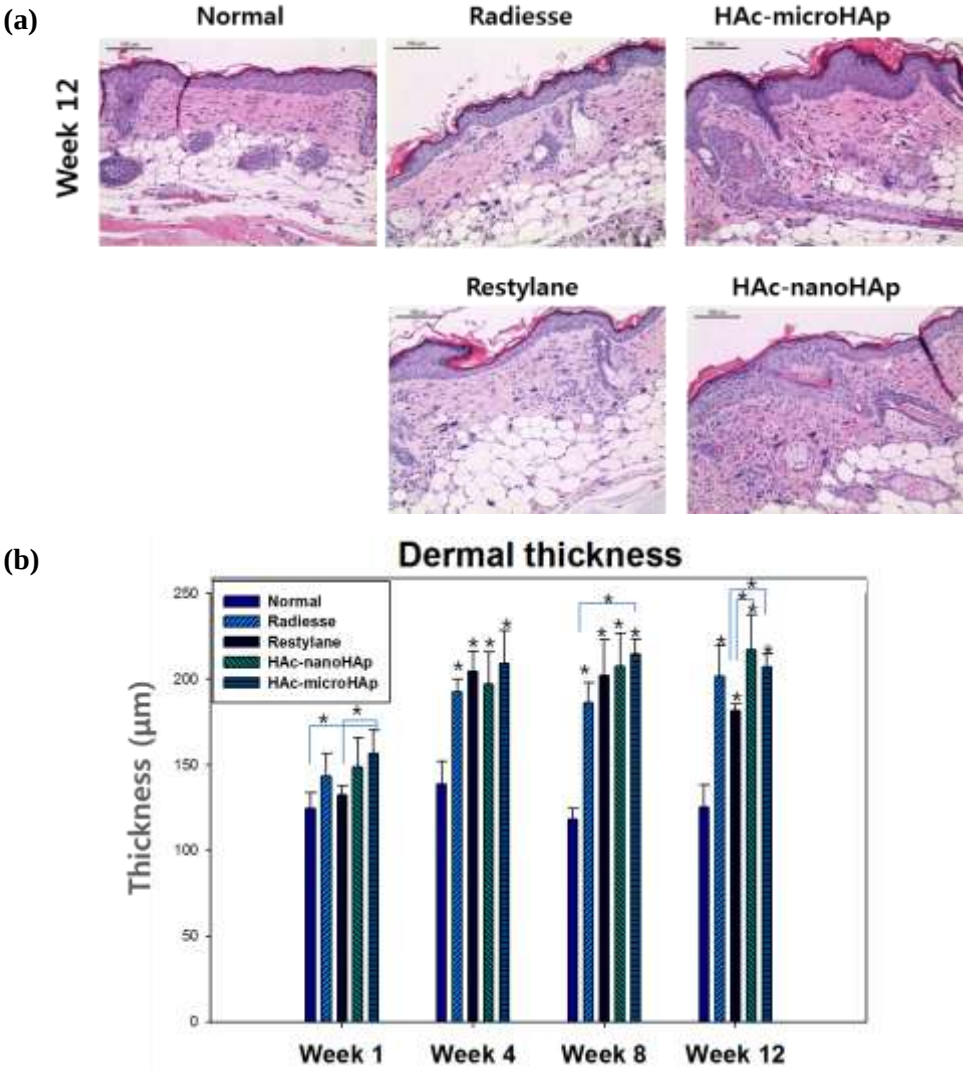

Figure 2. Skin dermal thickness assessed by hematoxylin and eosin (H&E) staining.

(a) Mouse skin samples stained with H&E stain at weeks 12. Scale bars = 100 μm. **(b)** Analysis of dermis thickness using ImageJ. Each measurement represents the mean ± SD. All filler groups showed a consistent increase in dermal thickness with age. At week 1, the HAc-microHAp group exhibited an initial increase. At week 12, the HAc-HAp group had a significantly greater thickness than the Restylane group (*$P < 0.01$).

The mechanism of collagen and elastic fiber formation

Cross-linked HAc filler increases the collagen via the TGF-ß/Smad pathway. It is associated with the upregulation of type II TGF-ß receptor and connected tissue growth factor. HAc facilitates TGF-ß1-dependent fibroblast proliferation by promoting the interaction between CD44 and EGFR, which then promotes MAPK/ERK phosphorylation, inducing cellular proliferation. Cross-linked HAc filler could also increase the elastic fiber content via the TGF-ß/Smad pathway and stimulate the expression of elastin and fibrillin. Smad7 is an inhibitor of the TGF-ß/Smad pathway, and prevented collagen and elastic fiber formation (Figure 3).

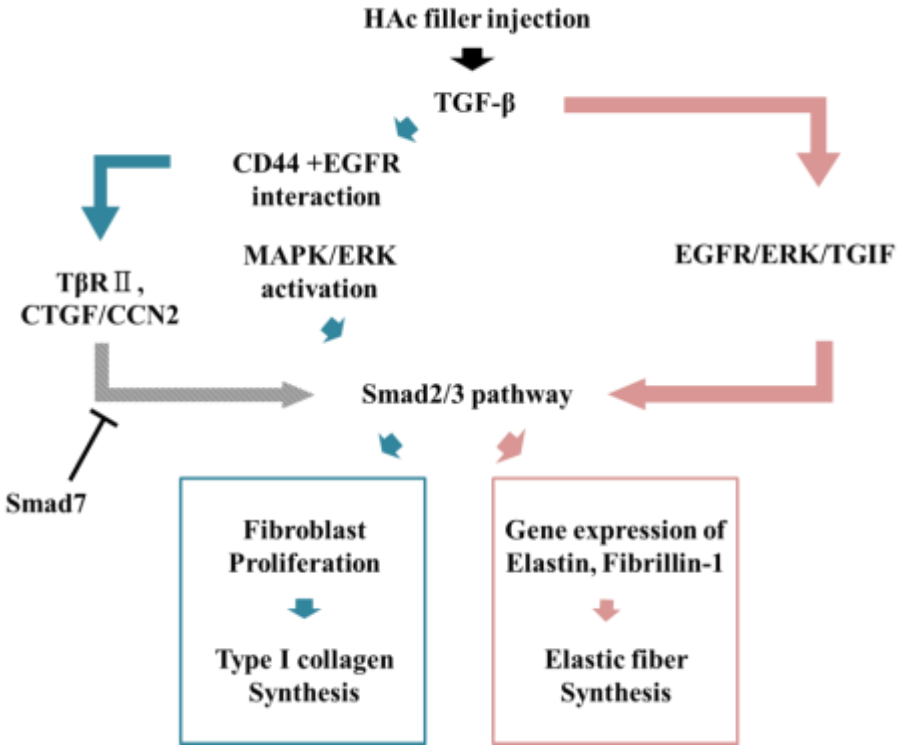

Figure 3. The mechanism of collagen and elastic fiber formation.

Cross-linked hyaluronic acid (HAc) filler increase collagen via the TGF-ß/Smad pathway. It is associated with the upregulation of type II TGF-ß receptor and connective tissue growth factor. HAc facilitates TGF-ß-dependent fibroblast proliferation by promoting the interaction between CD44 and EGFR, which then promotes MAPK/ERK phosphorylation, inducing cellular proliferation. Cross-linked HAc filler can also increase elastic fibers via the TGF-ß/Smad pathway and stimulation of the expression of elastin and fibrillin. Smad7 is an inhibitor of the TGF-ß/Smad pathway, and prevents collagen and elastic fiber formation.

Dermal collagen formation assessment

Dermal collagen formation after Radiesse and HAc-microHAp treatment

The collagen distribution determined using Masson's trichrome staining, is shown in Figure 4a. Collagen (represented by the blue area in the dermis in Figure 4a) was measured as the mean value of 5 different fields on a slide. At week 1, the HAc-microHAp group increased first, and had a significantly greater collagen area than the Radiesse group. At week 8, the collagen area of all filler groups were significantly increased, and maintained similar collagen levels after 12 weeks (Figure 4c) ($P < 0.01$). An immunohistochemistry analysis of vimentin, a fibroblast marker, was performed and the results are shown in Figure 4b. At week 1, the HAc-microHAp group increased first, and the vimentin levels in the HAc-microHAp increased significantly after 1, 4, and 8 weeks (Figure 4d) ($P < 0.01$). The mRNA levels of *EGFR*, *Smad2*, *Smad3*, and procollagen were assessed using real-time PCR after 4 and 12 weeks (Figure 4e). The *EGFR*, *Smad2*, and procollagen mRNA expression levels had similar patterns, and the procollagen levels were significantly higher in the HAc-microHAp groups than the Radiesse group ($P < 0.005$). The *Smad2* levels in the Radiesse and HAc-microHAp groups showed the opposite pattern compared with *Smad3* levels, and had significant differences in the expression of these genes ($P < 0.05$). No significant differences in the expression of any gene were observed between groups at week 12. The gene expression levels decreased at week 12. The protein expression levels of TGF-ß, EGFR, Smad2/3, collagen type 1, Smad7, and

phosphorylated MAPK (ERK1/2) were visualized by western blotting at 12 weeks after injections with fillers (Figure 4f). HAc-microHAp groups had similar levels of TGF-ß, EGFR, p-MAPK, Smad2/3, and collagen type 1, while Radiesse group did not. Smad7 is an inhibitor of the TGF-ß/Smad signaling pathway. Smad7 expression was not negatively correlated with the expression of the Smad2/3 proteins in the Radiesse and HAc-microHAp groups ($P < 0.05$).

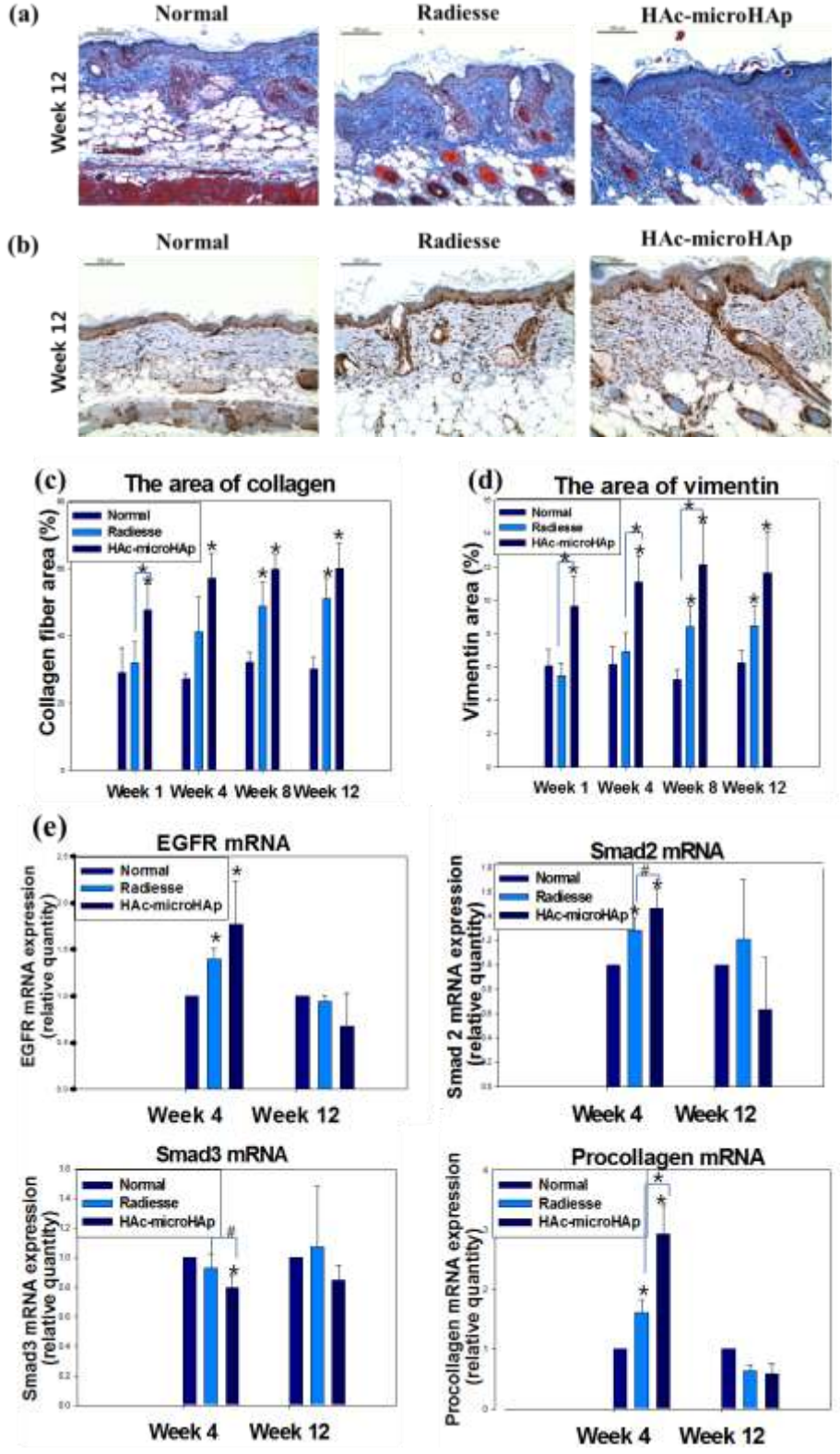
(a)
Normal
Radiesse
HAc-microHAp
Week 12
(b)
Normal
Radiesse
HAc-microHAp
Week 12
(c)
The area of collagen
Collagen fiber area (%)
Normal
Radiesse
HAc-microHAp
Week 1 Week 4 Week 8 Week 12
(d)
The area of vimentin
Vimentin area (%)
Normal
Radiesse
HAc-microHAp
Week 1 Week 4 Week 8 Week 12
(e)
EGFR mRNA
EGFR mRNA expression (relative quantity)
Normal
Radiesse
HAc-microHAp
Week 4 Week 12
Smad2 mRNA
Smad 2 mRNA expression (relative quantity)
Normal
Radiesse
HAc-microHAp
Week 4 Week 12
Smad3 mRNA
Smad3 mRNA expression (relative quantity)
Normal
Radiesse
HAc-microHAp
Week 4 Week 12
Procollagen mRNA
Procollagen mRNA expression (relative quantity)
Normal
Radiesse
HAc-microHAp
Week 4 Week 12

(f)

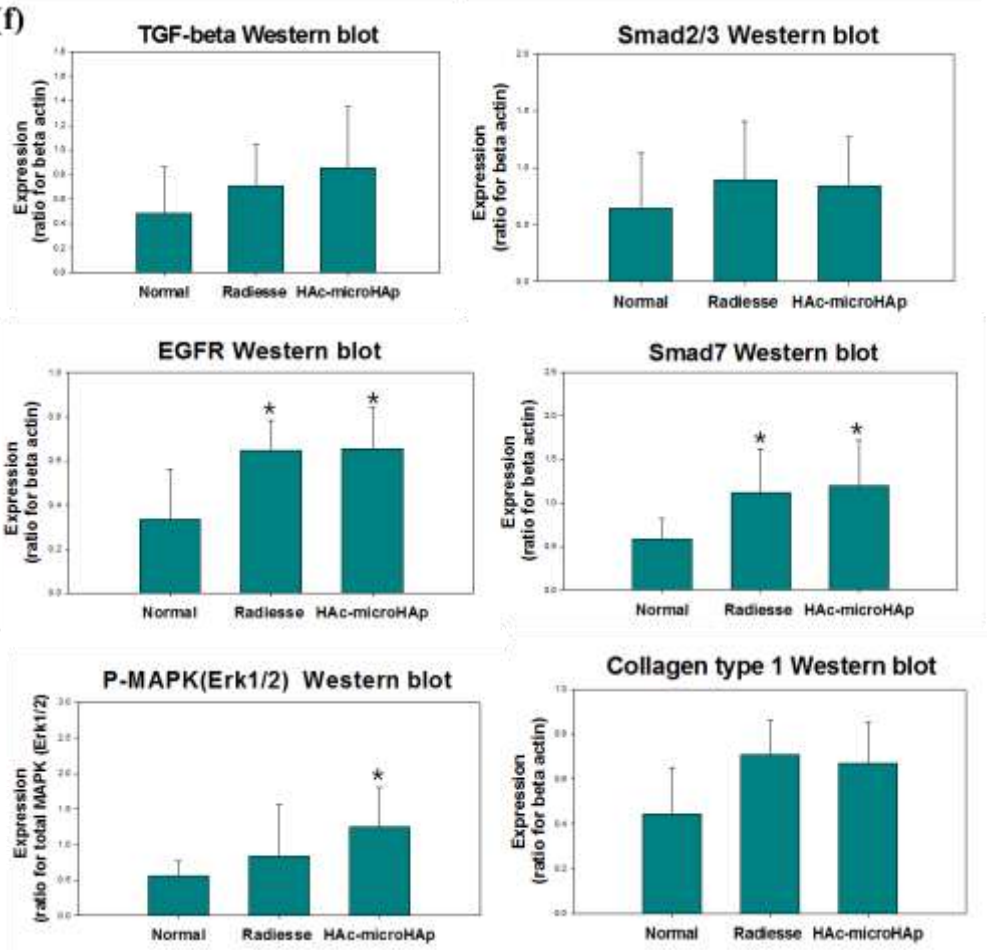
TGF-beta Western blot
Smad2/3 Western blot
EGFR Western blot
Smad7 Western blot
P-MAPK(Erk1/2) Western blot
Collagen type 1 Western blot
Expression (ratio for beta actin)
Expression (ratio for total MAPK (Erk1/2)
Normal
Radiesse
HAc-microHAp
*

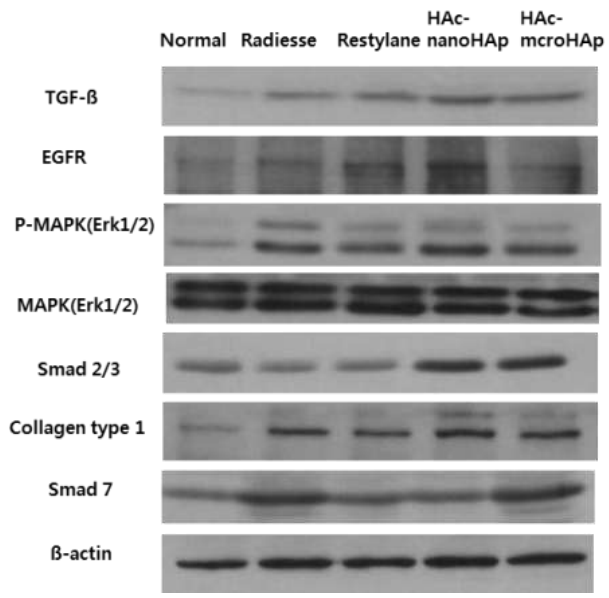
Normal
Radiesse
Restylane
HAc-nanoHAp
HAc-mcroHAp
TGF-ß
EGFR
P-MAPK(Erk1/2)
MAPK(Erk1/2)
Smad 2/3
Collagen type 1
Smad 7
ß-actin

Figure 4. Collagen formation in the Radiesse and HAc-microHAp groups.

(a) At 1, 4, 8, and 12 weeks, the collagen distribution was determined using Masson's trichrome staining; collagen fibers are stained blue. Scale bars = 100 μm. **(b)** The vimentin immunohistochemistry analysis was performed at 1, 4, 8, and 12 weeks after filler injection. Scale bars = 100 μm. **(c)** Collagen (blue area in the dermis) was measured as the mean value of 5 different fields on the same slide. Each measurement is presented as the mean ± SD. At week 1, the HAc-microHAp group increased first, and had a significantly greater collagen area than the Radiesse group. At week 8, the collagen area of all filler groups were significantly increased, and maintained similar collagen levels after 12 weeks (*$P < 0.01$). **(d)** Vimentin is a fibroblast marker. All measurements are expressed as the mean values and standard deviation of 5 different fields on the same slide. At week 1, the HAc-microHAp group increased first, and the vimentin levels in the HAc-microHAp increased significantly after 1, 4, and 8 weeks (*$P < 0.01$). **(e)** Real-time PCR was performed after 4 and 12 weeks. Each measurement is presented as the mean ± SD. The *EGFR*, *Smad2*, and procollagen mRNA expression levels had similar patterns, and the procollagen levels of the HAc-microHAp groups was significantly higher than the Radiesse group (*$P < 0.005$). The *Smad2* levels in the Radiesse and HAc-microHAp groups showed the opposite pattern compared with *Smad3* levels, and had significant differences in the expression of these genes ($P < 0.05$). No significant differences in the expression of any gene were observed between groups at week 12. The gene expression levels decreased at week 12. **(f)** Western blotting was performed at 12 weeks after filler injection. Quantification of the western blot data using a band-intensity densitometric analysis

in the striatum. Each measurement is presented as the mean ± SD. HAc-microHAp groups had similar levels of TGF-ß, EGFR, p-MAPK, Smad2/3, and collagen type 1, while the Radiesse group exhibited different expression levels. Smad7 is an inhibitor of the TGF-ß/Smad signaling pathway. Smad7 expression was not negatively correlated with the expression of the Smad2/3 proteins in the Radiesse and HAc-microHAp groups (*$P < 0.05$). # Statistically significant difference between the Radiesse and HAc-microHAp group ($P < 0.05$).

Dermal collagen formation after Restylane and HAc-nanoHAp treatment

The collagen distribution determined using Masson's trichrome staining, is shown in Figure 5a. Collagen (represented by the blue area in the dermis in Figure 5a) was measured as the mean value of 5 different fields on a slide. At week 4, the collagen area was increased significantly for the Restylane and HAc-nanoHAp group, and consistent increase with age. At week 12, The HAc-nanoHAp group had a significantly greater collagen area than the Restylane group (Figure 5c) ($P < 0.05$). An immunohistochemistry analysis of vimentin, a fibroblast marker, was performed and the results are shown in Figure 5b. The vimentin levels in the Restylane and HAc-nanoHAp groups increased significantly after 4 weeks, but did not exhibit additional changes after 8 and 12 weeks (Figure 5d) ($P < 0.05$). The mRNA levels of *EGFR*, *Smad2*, *Smad3*, and procollagen were assessed using real-time PCR after 4 and 12 weeks (Figure 5e). At week 4, the *EGFR*, *Smad2*, and procollagen mRNA expression levels had similar patterns except *Smad3*, no significant differences in the expression of *Smad3*. The *EGFR* levels of the HAc-nanoHAp groups was significantly higher than the Restylane group ($P < 0.005$). No significant differences in the expression of any gene were observed between groups at week 12. The gene expression levels decreased at week 12. The protein expression levels of TGF-ß, EGFR, Smad2/3, collagen type 1, Smad7, and phosphorylated MAPK (ERK1/2) were visualized by western blotting at 12 weeks after injections with fillers (Figure 5f). The Restylane and HAc-nanoHAp groups had similar levels of TGF-ß, EGFR, p-MAPK, Smad2/3, and collagen type 1. The EGFR, p-MAPK, and collagen type 1 level of the

HAc-nanoHAp groups increased significantly ($P < 0.005$). Smad7 is an inhibitor of the TGF-ß/Smad signaling pathway. Smad7 expression was negatively correlated with the expression of the Smad2/3 proteins in the Restylane and HAc-nanoHAp groups.

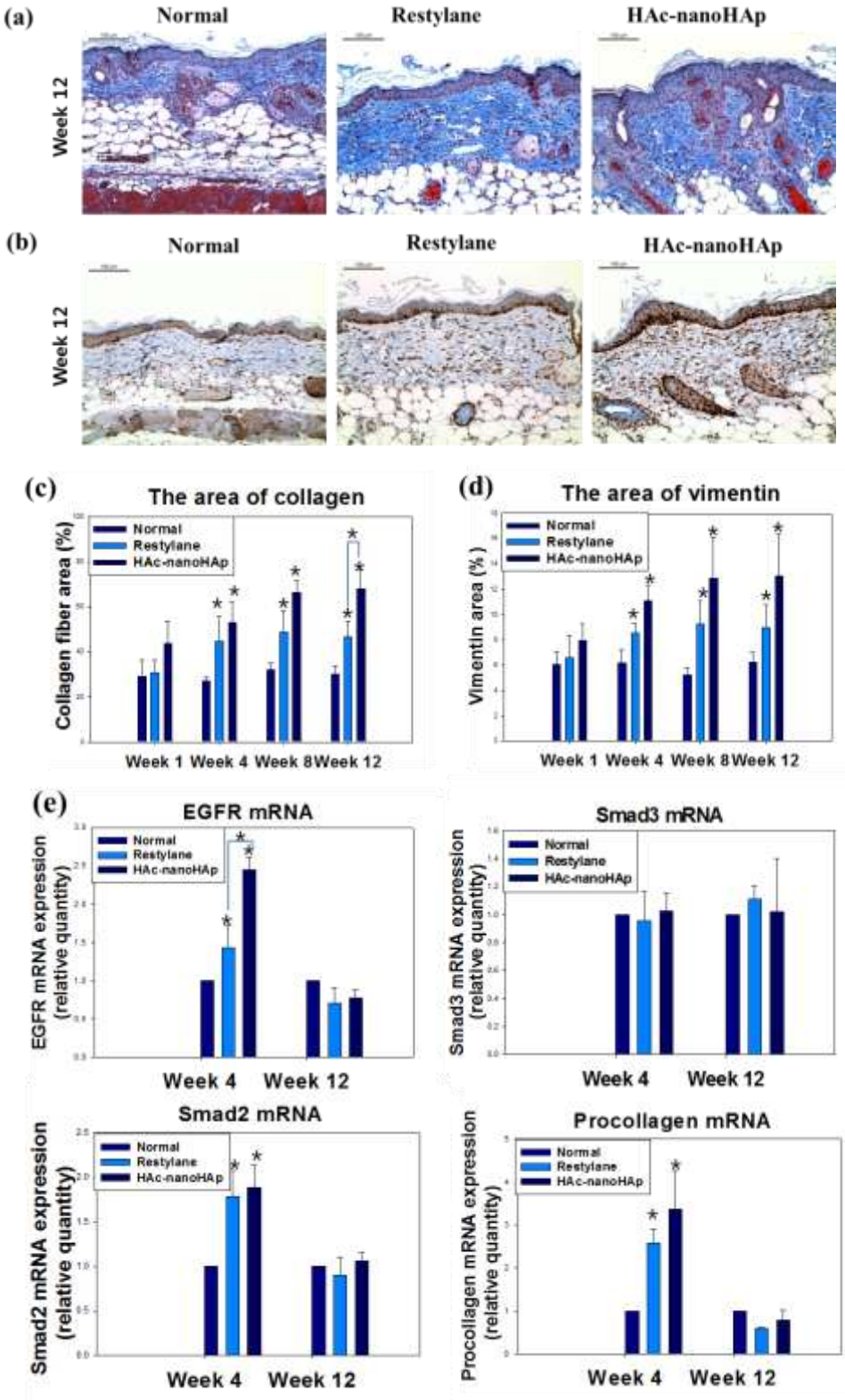
(a)
Normal
Restylane
HAc-nanoHAp
Week 12
(b)
Normal
Restylane
HAc-nanoHAp
Week 12
(c)
The area of collagen
Collagen fiber area (%)
Normal
Restylane
HAc-nanoHAp
Week 1 Week 4 Week 8 Week 12
(d)
The area of vimentin
Vimentin area (%)
Normal
Restylane
HAc-nanoHAp
Week 1 Week 4 Week 8 Week 12
(e)
EGFR mRNA
EGFR mRNA expression (relative quantity)
Normal
Restylane
HAc-nanoHAp
Week 4 Week 12
Smad3 mRNA
Smad3 mRNA expression (relative quantity)
Normal
Restylane
HAc-nanoHAp
Week 4 Week 12
Smad2 mRNA
Smad2 mRNA expression (relative quantity)
Normal
Restylane
HAc-nanoHAp
Week 4 Week 12
Procollagen mRNA
Procollagen mRNA expression (relative quantity)
Normal
Restylane
HAc-nanoHAp
Week 4 Week 12

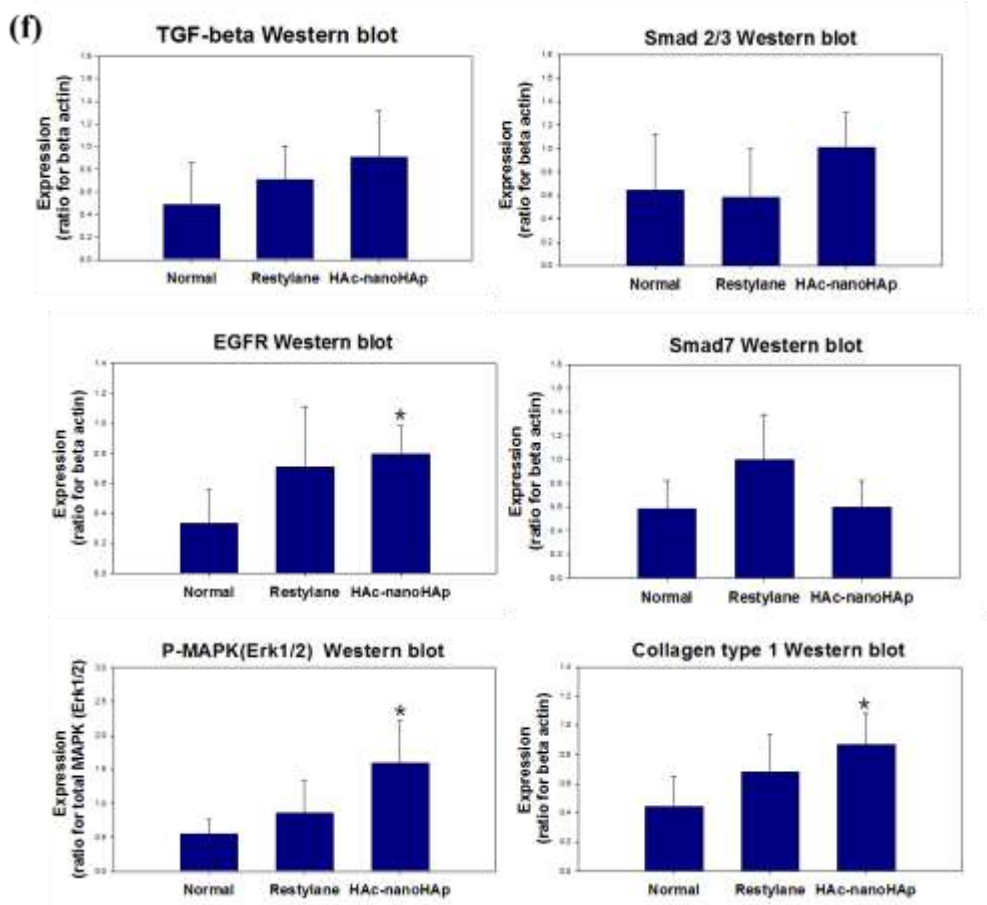

Figure 5. Collagen formation in the Restylane and HAc-nanoHAp groups.

(a) At 1, 4, 8, and 12 weeks, the collagen distribution was determined using Masson's trichrome staining; collagen fibers are stained blue. Scale bars = 100 μm. **(b)** The vimentin immunohistochemistry analysis was performed at 1, 4, 8, and 12 weeks after filler injection. Scale bars = 100 μm. **(c)** Collagen (blue area in the dermis) was measured as the mean value of 5 different fields on the same slide. Each measurement is presented as the mean ± SD. At week 4, the collagen area was increased significantly for the Restylane and HAc-nanoHAp group, and consistent increase with

age. At week 12, The HAc-nanoHAp group had a significantly greater collagen area than the Restylane group (*P < 0.05). **(d)** Vimentin is a fibroblast marker. All measurements are expressed as the mean values and standard deviation of 5 different fields on the same slide. The vimentin levels in the Restylane and HAc-nanoHAp groups increased significantly after 4 weeks, but did not exhibit additional changes after 8 and 12 weeks (*P < 0.05). **(e)** Real-time PCR was performed after 4 and 12 weeks. Each measurement is presented as the mean ± SD. At week 4, the *EGFR*, *Smad2*, and procollagen mRNA expression levels had similar patterns except *Smad3*, and there were no significant differences in the expression of *Smad3*. The *EGFR* levels of the HAc-nanoHAp group was significantly higher than the Restylane group (*P < 0.005). No significant differences in the expression of any gene were observed between groups at week 12. The gene expression levels decreased at week 12. **(f)** Western blotting was performed at 12 weeks after filler injection. Quantification of the western blot data using a band-intensity densitometric analysis in the striatum. Each measurement is presented as the mean ± SD. Restylane and HAc-nanoHAp groups had similar levels of TGF-ß, EGFR, p-MAPK, Smad2/3, and collagen type 1. The EGFR, p-MAPK and collagen type 1 level of the HAc-nanoHAp groups was increased significantly (*P < 0.005). Smad7 is an inhibitor of the TGF-ß/Smad signaling pathway. Smad7 expression was negatively correlated with the expression of the Smad2/3 proteins in the Restylane and HAc-nanoHAp groups.

Dermal elastic fiber formation assessment

Dermal elastic fiber formation after Radiesse and HAc-microHAp treatment

Elastic fibers were examined using Verhoeff-Van Gieson staining (Figure 6a). Elastic fiber (black area in the dermis) was measured as the mean value of 5 different fields on the same slide. At week 1, 4, 8, and 12, a significant increase in the dermal elastic fiber was observed after the filler injections. The elastic fiber area of the HAc-microHAp group was significantly larger than that of the Radiesse group at week 1 ($P < 0.01$; Figure 6c). A tropoelastin immune-histochemistry analysis was performed at weeks 1, 4, 8, and 12 and the results are summarized in Figure 6b. The tropoelastin levels of the Radiesse and HAc-microHAp groups increased significantly at weeks 1 and 8. At week 12, the tropoelastin levels of the HAc-microHAp group were significantly higher than those of the Radiesse group ($P < 0.01$; Figure 6d). The mRNA levels of *EGFR*, *Smad2*, *Smad3*, elastin, and fibrillin were assessed using real-time PCR after 4 and 12 weeks (Figure 6e). At week 4, the *EGFR*, *Smad2*, elastin and fibrillin mRNA expression levels of the two treatment groups increased significantly, except the fibrillin levels of the Radiesse group. The HAc-microHAp group exhibited similar patterns of gene expression, while the Radiesse group did not. The *smad2* and fibrillin levels of the HAc-microHAp groups were significantly higher than those of the Radiesse group ($P < 0.05$ and $P < 0.01$, respectively). No significant differences in the expression of any gene were observed between groups at week 12. The gene expression levels decreased at week 12.

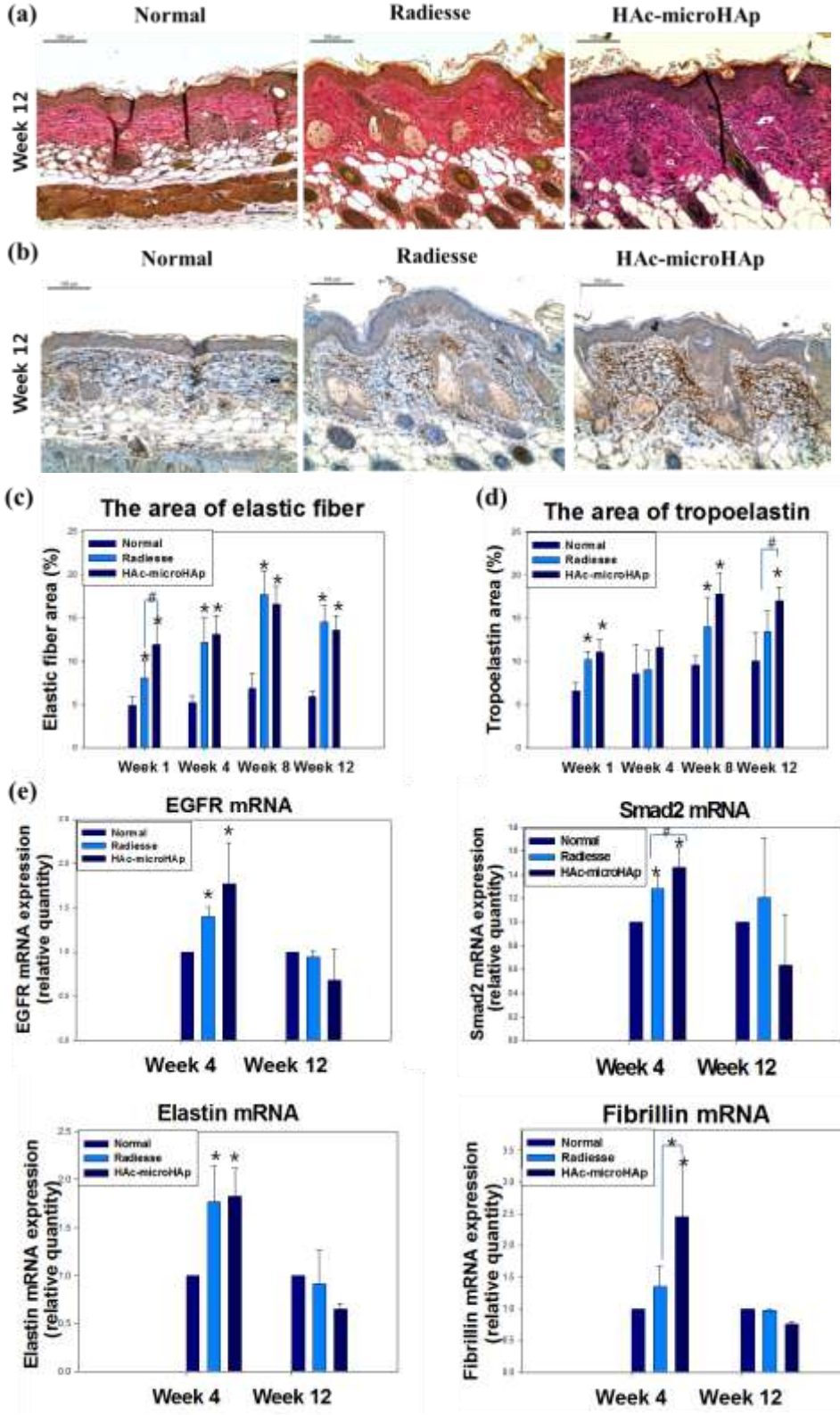
(a)
Normal
Radiesse
HAc-microHAp
Week 12
(b)
Normal
Radiesse
HAc-microHAp
Week 12
(c)
The area of elastic fiber
Elastic fiber area (%)
Normal
Radiesse
HAc-microHAp
Week 1 Week 4 Week 8 Week 12
(d)
The area of tropoelastin
Tropoelastin area (%)
Normal
Radiesse
HAc-microHAp
Week 1 Week 4 Week 8 Week 12
(e)
EGFR mRNA
EGFR mRNA expression (relative quantity)
Normal
Radiesse
HAc-microHAp
Week 4 Week 12
Smad2 mRNA
Smad2 mRNA expression (relative quantity)
Normal
Radiesse
HAc-microHAp
Week 4 Week 12
Elastin mRNA
Elastin mRNA expression (relative quantity)
Normal
Radiesse
HAc-microHAp
Week 4 Week 12
Fibrillin mRNA
Fibrillin mRNA expression (relative quantity)
Normal
Radiesse
HAc-microHAp
Week 4 Week 12

Figure 6. Elastic fiber formation in the Radiesse and HAc-microHAp groups.

(a) At 1, 4, 8, and 12 weeks, elastic fiber was examined using Verhoeff-Van Gieson staining, which stained the elastic fibers black. Scale bars = 100 μm. **(b)** The tropoelastin immunohistochemistry was performed at 1, 4, 8, and 12 weeks after filler injections. Scale bars = 100 μm. **(c)** Elastic fiber (black area in the dermis) was measured as the mean value of 5 different fields on the same slide. Each measurement is presented as the mean ± SD. At week 1, 4, 8, and 12, a significant increase in the dermal elastic fiber was observed after the filler injections. The elastic fiber area of the HAc-microHAp group was significantly larger than that of the Radiesse group at week 1 (*P < 0.01). **(d)** All measurements are expressed as the mean values and standard deviations of 5 different fields on the same slide. The tropoelastin levels of Radiesse and HAc-microHAp groups were increased significantly at week 1 and 8. At week 12, the tropoelastin levels of the HAc-microHAp group were significantly higher than those of the Radiesse group (*P < 0.01). **(e)** Real-time PCR was performed after 4 and 12 weeks. At week 4, the *EGFR*, *Smad2*, elastin and fibrillin mRNA expression levels of the two treatment groups were increased significantly except the fibrillin of Radiesse group. The HAc-microHAp group exhibited similar patterns of gene expression, while the Radiesse group did not. The *Smad2* and fibrillin levels of the HAc-microHAp groups were significantly higher than the Radiesse group (P < 0.05 and *P < 0.01, respectively). No significant differences in the expression of any gene were observed between groups at week 12. The gene expression levels decreased at week 12. # Statistically significant difference between the Radiesse and HAc-microHAp group (P < 0.05).

Dermal elastic fiber formation after Restylane and HAc-nanoHAp treatment

Elastic fibers were examined using Verhoeff-Van Gieson staining (Figure 7a). Elastic fiber (black area in the dermis) was measured as the mean value of 5 different fields on the same slide. At week 1, 4, 8, and 12, a significant increase in the dermal elastic fiber was observed after the filler injections. The elastic fiber area of the HAc-nanoHAp group was significantly larger than that of the Restylane group at week 4 (Figure 7c) ($P < 0.01$). A tropoelastin immunohistochemistry analysis was performed at weeks 1, 4, 8, and 12 and the results are summarized in Figure 7b. The tropoelastin levels of the Restylane and HAc-nanoHAp groups increased significantly at week 1. At weeks 8 and 12, the tropoelastin levels of the HAc-nanoHAp group were significantly higher than those of the Restylane group, and the two filler groups maintained similar tropoelastin levels after 12 weeks (Figure 7d) ($P < 0.01$). The mRNA levels of *EGFR*, *Smad2*, *Smad3*, elastin, and fibrillin were assessed using real-time PCR after 4 and 12 weeks (Figure 7e). At week 4, the *EGFR*, *Smad2*, elastin, and fibrillin mRNA expression levels of the two treatment groups were increased significantly, and they exhibited similar patterns of gene expression. The *EGFR* and elastin levels were significantly higher in the HAc-nanoHAp groups than the Restylane group ($P < 0.005$). No significant differences in the expression of any gene were observed between groups at week 12. The gene expression levels decreased at week 12.

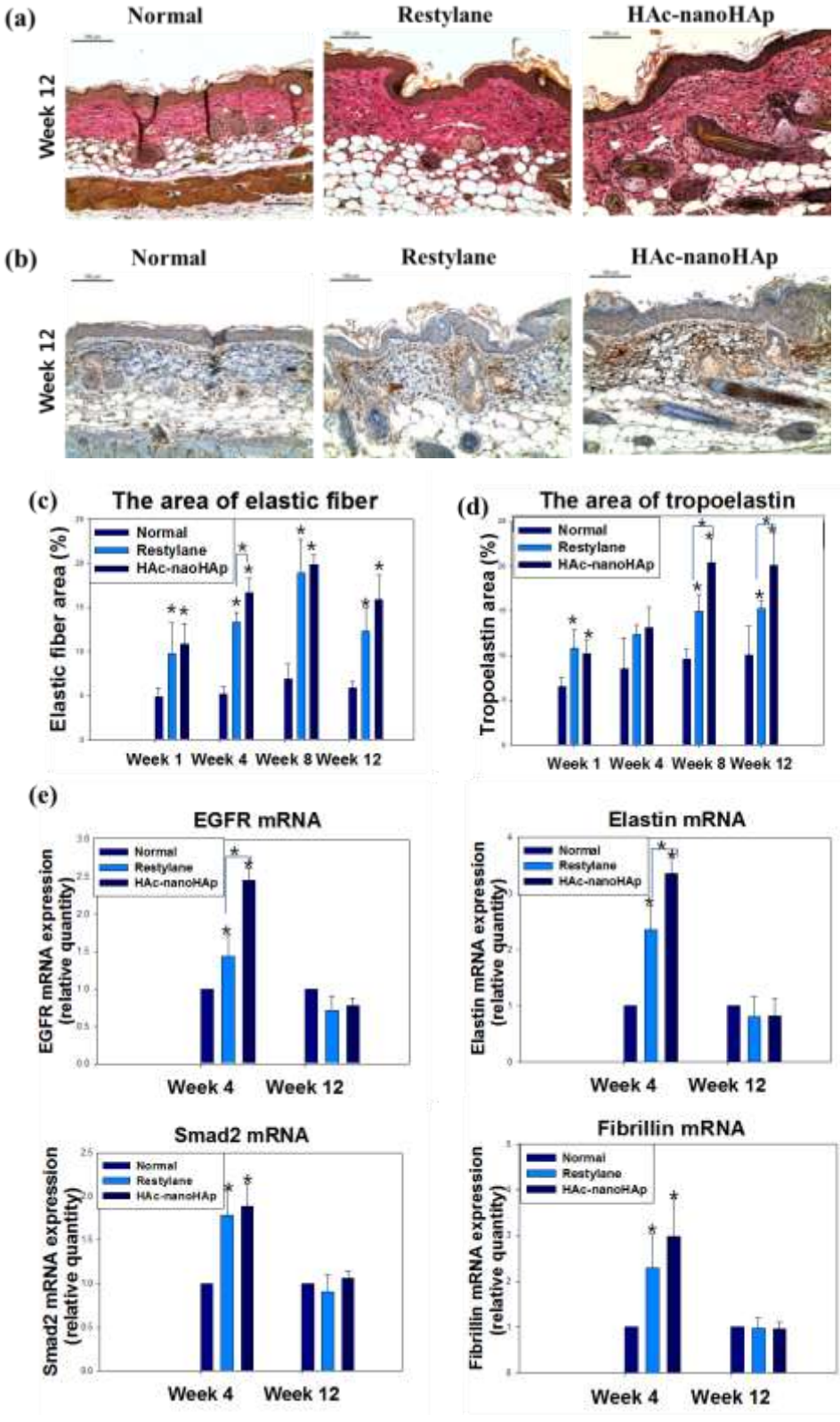
(a)
Normal
Restylane
HAc-nanoHAp
Week 12
(b)
Normal
Restylane
HAc-nanoHAp
Week 12
(c)
The area of elastic fiber
Elastic fiber area (%)
Normal
Restylane
HAc-naoHAp
Week 1 Week 4 Week 8 Week 12
(d)
The area of tropoelastin
Tropoelastin area (%)
Normal
Restylane
HAc-nanoHAp
Week 1 Week 4 Week 8 Week 12
(e)
EGFR mRNA
EGFR mRNA expression (relative quantity)
Normal
Restylane
HAc-nanoHAp
Week 4 Week 12
Elastin mRNA
Elastin mRNA expression (relative quantity)
Normal
Restylane
HAc-nanoHAp
Week 4 Week 12
Smad2 mRNA
Smad2 mRNA expression (relative quantity)
Normal
Restylane
HAc-nanoHAp
Week 4 Week 12
Fibrillin mRNA
Fibrillin mRNA expression (relative quantity)
Normal
Restylane
HAc-nanoHAp
Week 4 Week 12

Figure 7. Elastic fiber formation in the Restylane and HAc-nanoHAp groups.

(a) At 1, 4, 8, and 12 weeks, elastic fiber was examined using Verhoeff-Van Gieson staining, which stained the elastic fibers black. Scale bars = 100 μm. **(b)** The tropoelastin immunohistochemistry was performed at 1, 4, 8, and 12 weeks after filler injections. Scale bars = 100 μm. **(c)** Elastic fiber (black area in the dermis) was measured as the mean value of 5 different fields on the same slide. Each measurement is presented as the mean ± SD. At week 1, 4, 8, and 12, a significant increase in the dermal elastic fiber was observed after the filler injections. The elastic fiber area of the HAc-nanoHAp group was significantly larger than that of the Restylane group at week 4 (*P < 0.01). **(d)** All measurements are expressed as the mean values and standard deviations of 5 different fields on the same slide. The tropoelastin levels of Restylane and HAc-nanoHAp groups were increased significantly at week 1. At week 8 and 12, the tropoelastin levels of the HAc-nanoHAp group were significantly higher than those of the Restylane group, and the two filler groups maintained similar tropoelastin levels after 12 weeks (*P < 0.01). **(e)** Real-time PCR was performed after 4 and 12 weeks. Each measurement is presented as the mean ± SD. At week 4, the *EGFR*, *Smad2*, elastin and fibrillin mRNA expression levels of the two treatment groups increased significantly, and they exhibited similar patterns of gene expression. The *EGFR* and elastin levels of the HAc-nanoHAp groups were significantly higher than those of the Restylane group (*P < 0.005). No significant differences in the expression of any gene were observed between groups at week 12. The gene expression levels decreased at week 12.

Nanoparticle safety

The kidney, liver, lung, and spleen were stained with H&E at week 12. Based on H&E staining, there was no organ damage, structural malformation, or necrosis. Additionally, there was no abnormal inflammatory cell infiltration and no abnormal increase in macrophages in any of the organs (Figure 8).

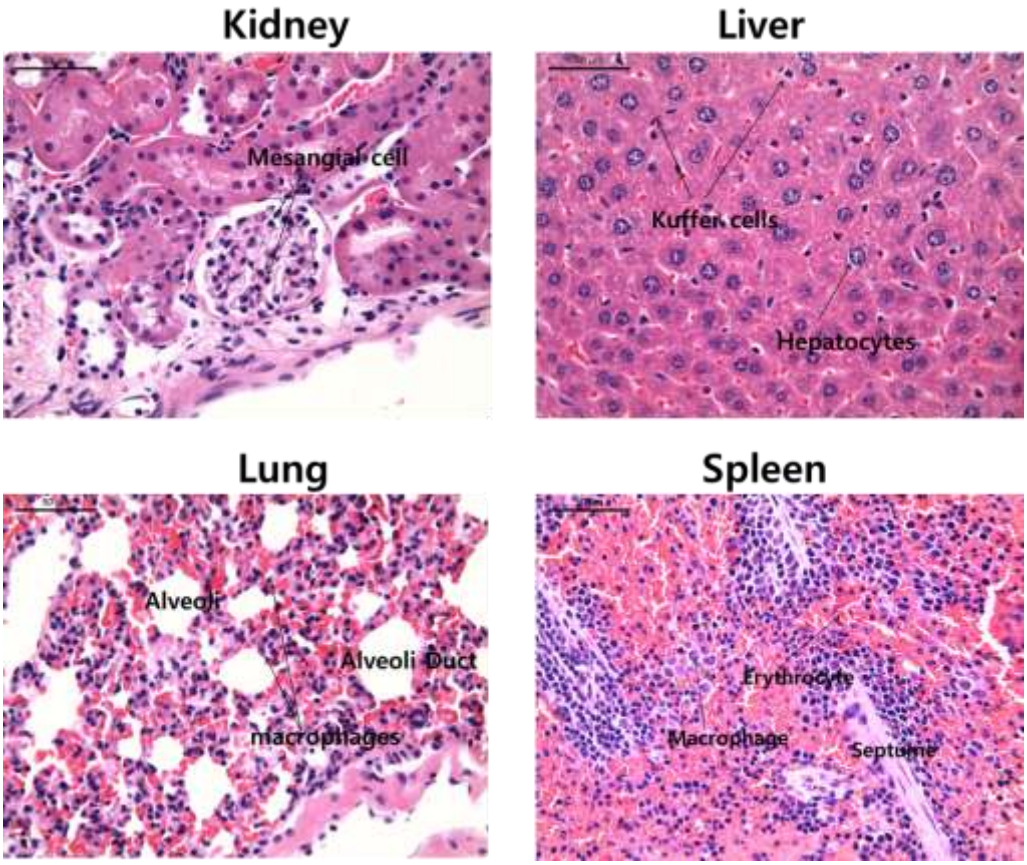

Figure 8. Organ toxicity of filler nanoparticles based on an H&E analysis.

The kidney, liver, lung, and spleen were stained with H&E at week 12. Scale bars = 50 μm. H&E staining showed that there was no organ damage, structural malformation, or necrosis; additionally, there was no abnormal inflammatory cell infiltration or increase in macrophages in any organ.

DISCUSSION

HAc filler is the most common dermal injection (3, 6, 20). Cross-linked HAc fillers increase dermal thickness and extracellular matrix components (1, 4, 21). CaHA can also stimulate increases in collagen and elastic fibers (16, 17). The CaHA Radiesse is highly effective with respect to improving facial contours (4, 22-24); accordingly, it is very popular. However, its longevity is insufficient owing to its biodegradability (24). In the nude mouse model used in this study, the longevity of the HAc-HAp composite filler and its effects on collagen and elastic fiber synthesis were demonstrated.

Imaging and MRI volumetric analyses revealed that the HAc-HAp composite filler had better longevity than pure HAc and pure HAp. The HAc-nanoHAp group had better stability than the other 3 groups. The HAc-HAp composite filler included 70% HAc as a matrix and 30% HAp as a reinforcer. HAp can enhance the stability of HAc, which has a degree of stability when used alone. Radiesse consists of 30% CaHA in a 70% aqueous CMC gel carrier (1, 6). CMC is used in the pharmaceutical industry as an excipient and for drug delivery (7-9). In the HAc-HAp composite filler, HAc was not only used as excipient, but also as stabilizer; HAp enables fibroblastic integration and collagen deposition in and around the implant (25). Therefore, the HAc-HAp composite filler lasted longer than Restylane and Radiesse.

All filler groups consistently showed increases in dermal thickness with age. At week

1, the HAc-microHAp group first exhibited an increase. At week 12, the HAc-HAp group had a significantly greater dermal thickness than the Restylane group. There are several explanations for the increase in skin thickness. We focused on changes in collagen and elastic fibers.

In a comparison between the Radiesse and HAc-microHAp group, at week 1, the collagen level of HAc-microHAp group increased, and was significantly greater than it was in the Radiesse group. This is consistent with the results for skin thickness. The proportions of HAp on Radiesse and HAc-microHAp were the same, and CMC does not have the ability to promote collagen formation, while HAc itself does promote collagen formation. Therefore, HAc-microHAp produced more collagen than Radiesse. At week 8, the collagen areas of all filler groups increased significantly, and similar collagen levels were maintained after 12 weeks. Because genetic growth should be most obvious in the previous stage, we analyzed genetic changes at week 4. The *EGFR*, *Smad2*, and procollagen mRNA expression levels had similar patterns at week 4, and the procollagen levels were significantly higher in the HAc-microHAp groups than the Radiesse group. These results suggest that HAc collagen formation occurs via *EGFR* and *Smad2*. The *Smad2* levels in the Radiesse and HAc-microHAp groups showed the opposite pattern compared with *Smad3* levels, and there were significant differences between the expression levels of these genes. In the extracellular matrix environment, Smad2 can inhibit increases in Smad3, in the same way that Smad3 can inhibit increases in Smad2 (26). No significant differences in the expression of any gene were observed between groups at week 12. The gene

expression levels decreased at week 12. Despite the filler remaining in the skin, over time, the genes no longer increased. The western blot results showed that the HAc-microHAp groups had similar levels of TGF-ß, EGFR, p-MAPK, Smad2/3, and collagen type 1, while the Radiesse group exhibited clear differences. This suggests that HAc collagen formation is mediated by TGF-ß, EGFR, p-MAPK, Smad2/3, and collagen type 1. Vimentin is a fibroblast marker (27, 28). The vimentin levels in the HAc-microHAp increased significantly after 1, 4, and 8 weeks. This suggests that the fibroblasts in the HAc-microHAp group increased significantly. This is consistent with the results for dermal thickness and collagen area. It also supports the hypothesis summarized in Figure 3. It is not clear whether Radiesse induces collagen formation via the TGF-ß/Smad pathway. Some studies have shown that HAp injected into living bone promotes new bone formation via osteoblasts and osteoclasts (25). The hydroxyapatite scaffold is similar to the natural bone extracellular matrix, and promotes bone regeneration via the BMP/Smad pathway (29). When injected into soft tissue, HAp induces new collagen formation by fibroblast activation (17, 25). However, the specific pathway is not clear.

In a comparison between the Restylane and HAc-nanoHAp group, at week 4, the collagen area increased significantly in the Restylane and HAc-nanoHAp group, and the observed increases over time were consistent with the vimentin results. At week 12, the HAc-nanoHAp group had a significantly greater collagen area than the Restylane group. Restylane is HAc (20 mg/ml). The HAc-nanoHAp composite filler included 70% HAc and 30% HAp, while less than 100% HAc comprised the

Restylane filler. Both HAc and HAp have the ability to promote collagen formation. Therefore, the 100% HAc-nanoHAp composite filler produced more collagen than Restylane, which had less than 100% HAc. The *EGFR*, *Smad2*, and procollagen mRNA expression levels had similar patterns at week 4, and the Restylane and HAc-nanoHAp groups had similar protein levels of TGF-ß, EGFR, p-MAPK, Smad2/3, and collagen type 1 at week 12. These results proved that HAc promotes collagen formation via the TGF-ß/Smad signaling pathway. No significant differences were observed between groups in the expression of *Smad3*. Accordingly, Smad2 plays a primary role in the HAc-induced TGF-ß/Smad signaling pathway. The protein expression level of Smad7, an inhibitor of the TGF-ß/Smad pathway (30), increased in the Restylane group. This suggests that Smad7 expression was negatively correlated with the expression of the Smad2/3 proteins in the Restylane and HAc-nanoHAp groups. This provides further support for the hypothesis described in Figure 3. These results are consistent with changes in gene expression and protein generation resulting in collagen fiber assembly in skin tissues.

In a comparison between the Radiesse and HAc-microHAp group with respect to elastic fiber formation, there was a significant increase after the filler injections. The elastic fiber area of the HAc-microHAp group was significantly larger than that of the Radiesse group at week 1. This is consistent with the results for dermal thickness and collagen formation. HAc promotes collagen and elastic fiber formation by the same TGF-ß/Smad pathway. In the last week of the study, elastic fiber was not greater in the HAc-microHAp than the Radiesse group, but tropoelastin levels were

significantly higher than those of the Radiesse group. In particular, the *Smad2* and fibrillin levels were significantly higher in the HAc-microHAp groups than the Radiesse group at week 4. This provides direct and indirect proof that HAc-microHAp can better promote elastic fiber formation. At week 4, the *EGFR*, *Smad2*, elastin and fibrillin mRNA expression levels of the two treatment groups increased significantly, except the fibrillin levels of the Radiesse group. The HAc-microHAp group exhibited similar patterns of gene expression, while the Radiesse group did not. As mentioned above, Radiesse promotes collagen growth by another signaling pathway; thus, elastic fiber growth may be mediated by another pathway. Some studies have shown that collagen and elastic fiber formation induced by HAp are associated with collagen and elastic fiber remodeling and production (24, 31). No significant differences in the expression of any gene were observed between groups at week 12. Like collagen, although the filler remained in the skin, gene expression was no longer stimulated.

In a comparison between the Restylane and HAc-nanoHAp group with respect to elastic fiber formation, there was a significant increase at week 1 and these levels were maintained for 12 weeks. Although the elastic fiber decreased in all filler groups at week 12, the HAc-nanoHAp group generally exhibited greater increases in elastic fibers than the Restylane groups. Elastic fiber has two distinct components: microfibrils and elastin (12). Tropoelastin is a precursor of elastin and fibrillin-1 is a major component of the microfibrils within elastic fibers (32, 33). The tropoelastin levels of Restylane and HAc-nanoHAp groups increased significantly at week 1, and

the tropoelastin levels of the HAc-nanoHAp group were significantly higher than those of the Restylane group at weeks 8 and 12. Additionally, the two HAc groups had similar trends with respect to *EGFR, Smad2,* elastin, and fibrillin gene expression. The formation of elastic fiber is related to TGF-ß (13), supporting our hypothesis that the HAc filler stimulates an elastic fiber increase via the TGF-ß/Smad pathway (Figure 3).

The diameter (1–10 nm) of the NPs may stimulate cytotoxicity via direct effects on chromosomes, ribosomes, and membranes (34). HAp NPs of <50 nm are nontoxic at the cellular level (35). Although the HAc-nanoHAp NPs were 200 nm, their cytotoxicity was still examined in the kidney, liver, lung, and spleen. Based on H&E staining, there was no evidence of organ damage, structural malformation, or necrosis. Additionally, there was no abnormal inflammatory cell infiltration and no abnormal increase in macrophages in any organ.

These data support the hypothesized collagen and elastic fiber mechanism. The HAc-HAp filler can effectively increase collagen and elastic fibers and enhance the longevity of the filler. We injected the filler between the panniculus adiposus layer and panniculus carnosus. It effectively stimulated connective and fat tissue to produce collagen. These results validate the hypothesis that HAc-HAp composite filler promotes collagen and elastic fiber regeneration from genes to proteins, resulting in collagen and elastic fiber assembly in the skin tissue. The longevity of HAp is not due to the presence of microspheres, but rather collagen formation (24). The HAc-HAp

group exhibited greater increases in collagen than the Radiesse and Restylane groups, resulting in an extended effect.

CONCLUSION

The HAc-HAp composite filler promotes more collagen and elastic fiber regeneration than currently available pure fillers. This composite filler also has better longevity. Accordingly, this newly formulated HAc-HAp composite filler is a better option for correcting cosmetic problems, such as wrinkles. Further research should focus on the role of HAc-HAp composite fillers in photoaging in animal models, and their effects on physical properties of the skin, such as elasticity and tension strength.

REFERENCES

1. Iannitti T, Morales-Medina JC, Coacci A, Palmieri B. Experimental and Clinical Efficacy of Two Hyaluronic Acid-based Compounds of Different Cross-Linkage and Composition in the Rejuvenation of the Skin. Pharm. Res. 2014, Epub.
2. Kim ZH, Lee Y, Kim SM, Kim H, Yun CK, Choi YS. A composite dermal filler comprising cross-linked hyaluronic acid and human collagen for tissue reconstruction. J. Microbiol. Biotech. 2015;25(3):399-406.
3. Paliwal S, Fagien S, Sun X, Holt T, Kim T, Hee CK, et al. Skin extracellular matrix stimulation following injection of a hyaluronic acid-based dermal filler in a rat model. Plast. Reconstr. Surg. 2014;134(6):1224-1233.
4. Loghem JV, Yutskovskaya YA, Philip Werschler W. Calcium hydroxylapatite: over a decade of clinical experience. J. Clin. Aesth. Derm. 2015;8(1):38-49.
5. Varma DM, Gold GT, Taub PJ, Nicoll SB. Injectable carboxymethylcellulose hydrogels for soft tissue filler applications. Acta Biomater. 2014;10(12):4996-5004.
6. Redbord KP, Busso M, Hanke CW. Soft-tissue augmentation with hyaluronic acid and calcium hydroxyl apatite fillers. Derm. Ther. 2011;24(1):71-81.

7. Beasley KL, Weiss MA, Weiss RA. Hyaluronic acid fillers: a comprehensive review. Facial Plast. Surg. 2009;25(2):86-94.

8. Quan T, Wang F, Shao Y, Rittie L, Xia W, Orringer JS, et al. Enhancing structural support of the dermal microenvironment activates fibroblasts, endothelial cells, and keratinocytes in aged human skin in vivo. J. Invest. Derm. 2013;133(3):658-667.

9. Quan T, He T, Kang S, Voorhees JJ, Fisher GJ. Solar ultraviolet irradiation reduces collagen in photoaged human skin by blocking transforming growth factor-beta type II receptor/Smad signaling. Am. J. Pathol. 2004;165(3):741-751.

10. Son ED, Lee JY, Lee S, Kim MS, Lee BG, Chang IS, et al. Topical application of 17 beta-estradiol increases extracellular matrix protein synthesis by stimulating TGF-beta signaling in aged human skin in vivo. J. Invest. Derm. 2005;124(6):1149-1161.

11. Meran S, Luo DD, Simpson R, Martin J, Wells A, Steadman R, et al. Hyaluronan Facilitates Transforming Growth Factor-beta 1-dependent Proliferation via CD44 and Epidermal Growth Factor Receptor Interaction. J. Biol. Chem. 2011;286(20):17618-17630.

12. Kielty CM, Sherratt MJ, Shuttleworth CA. Elastic fibres. J. Cell Sci. 2002;115(Pt 14):2817-2828.

13. Urban Z, Davis EC. Cutis laxa: Intersection of elastic fiber biogenesis, TGF beta signaling, the secretory pathway and metabolism. Matrix Biol. 2014;33:16-22.

14. Sattler G, Walker T, Buxmeyer B, Biwer B. Efficacy of Calcium Hydroxylapatite Filler versus Hyaluronic Acid Filler in Hand Augmentation. Aktuelle Dermatologie. 2014;40(11):445-451.

15. Emer J, Sundaram H. Aesthetic applications of calcium hydroxylapatite volumizing filler: an evidence-based review and discussion of current concepts: (part 1 of 2). J. Drugs Derm. 2013;12(12):1345-1354.

16. Graivier MH, Bass LS, Busso M, Jasin ME, Narins RS, Tzikas TL. Calcium hydroxylapatite (Radiesse) for correction of the mid- and lower face: consensus recommendations. Plast. Reconstr. Surg. 2007;120(6 Suppl):55S-66S.

17. Marmur ES, Phelps R, Goldberg DJ. Clinical, histologic and electron microscopic findings after injection of a calcium hydroxylapatite filler. J. Cosmet. Laser Ther. 2004;6(4):223-226.

18. Leonardis M, Palange A. New-generation filler based on cross-linked carboxymethylcellulose: study of 350 patients with 3-year follow-up. Clin. Interv. Aging. 2015;10:147-155.

19. Barbucci R, Leone G, Vecchiullo A. Novel carboxymethylcellulose-based microporous hydrogels suitable for drug delivery. J. Biomater. Sci. Polymer Ed. 2004;15(5):607-619.

20. Duranti F, Salti G, Bovani B, Calandra M, Rosati ML. Injectable hyaluronic acid gel for soft tissue augmentation. A clinical and histological study. Derm. Surg. 1998;24(12):1317-1325.

21. Turlier V, Delalleau A, Casas C, Rouquier A, Bianchi P, Alvarez S, et al.

Association between collagen production and mechanical stretching in dermal extracellular matrix: In vivo effect of cross-linked hyaluronic acid filler. A randomised, placebo-controlled study. J. Dermatol. Sci. 2013;69(3):187-194.

22. Bernardini FP, Cetinkaya A, Devoto MH, Zambelli A. Calcium Hydroxyl-Apatite (Radiesse) for the Correction of Periorbital Hollows, Dark Circles, and Lower Eyelid Bags. Ophthal. Plast. Recons. 2014;30(1):34-39.

23. Buchanan AG, Holds JB, Vagefi MR, Bidar M, McCann JD, Anderson RL. Anterior Filler Displacement Following Injection of Calcium Hydroxylapatite Gel (Radiesse) for Anophthalmic Orbital Volume Augmentation. Ophthal. Plast. Recons. 2012;28(5):335-337.

24. Pavicic T. Complete biodegradable nature of calcium hydroxylapatite after injection for malar enhancement: an MRI study. Clin. Cosmet. Investigat. Dermatol. 2015;8:19-25.

25. Jansen DA, Graivier MH. Evaluation of a calcium hydroxylapatite-based implant (Radiesse) for facial soft-tissue augmentation. Plast. Reconstr. Surg. 2006;118(3 Suppl):22S-30S, discussion 1S-3S.

26. Li J, Tang X, Chen X. Comparative effects of TGF-β2/Smad2 and TGF-β2/Smad3 signaling pathways on proliferation, migration, and extracellular matrix production in a human lens cell line. Exp. Eye Res. 2011;92(3):173-179.

27. Goodpaster T, Legesse-Miller A, Harneed MR, Aisner SC, Randolph-Habecker J, Coller HA. An immunohistochemical method for identifying

fibroblasts in formalin-fixed, paraffin-embedded tissue. J. Histochem. Cytochem. 2008;56(4):347-358.

28. Pilling D, Fan T, Huang D, Kaul B, Gomer RH. Identification of Markers that Distinguish Monocyte-Derived Fibrocytes from Monocytes, Macrophages, and Fibroblasts. Plos One. 2009;4(10).

29. Liu HH, Peng HJ, Wu Y, Zhang C, Cai YZ, Xu GW, et al. The promotion of bone regeneration by nanofibrous hydroxyapatite/chitosan scaffolds by effects on integrin-BMP/Smad signaling pathway in BMSCs. Biomaterials. 2013;34(18):4404-4417.

30. Wang ZH, Zhang QS, Duan YL, Zhang JL, Li GF, Zheng DL. TGF-beta induced miR-132 enhances the activation of TGF-beta signaling through inhibiting SMAD7 expression in glioma cells. Biochem. Bioph. Res. Co. 2015;463(3):187-192.

31. Yutskovskaya Y, Kogan E, Leshunov E. A Randomized, Split-Face, Histomorphologic Study Comparing a Volumetric Calcium Hydroxylapatite and a Hyaluronic Acid-Based Dermal Filler. J. Drugs Dermatol. 2014;13(9):1047-1052.

32. Chen Z, Zhuo FL, Zhang SJ, Tian Y, Tian S, Zhang JZ. Modulation of tropoelastin and fibrillin-1 by infrared radiation in human skin in vivo. Photodermatol. Photo. 2009;25(6):310-316.

33. Mithieux SM, Weiss AS. Elastin. Adv. Prot. Chem. 2005;70:437-461.

34. Magrez A, Kasas S, Salicio V, Pasquier N, Seo JW, Celio M, et al. Cellular toxicity of carbon-based nanomaterials. Nano Lett. 2006;6(6):1121-1125.

35. Parayanthala Valappil M, Santhakumar S, Arumugam S. Determination of oxidative stress related toxicity on repeated dermal exposure of hydroxyapatite nanoparticles in rats. Int. J. Biomater. 2014;2014:476942.

국문 초록

서론: 누드마우스 모델에서 hyaluronic acid-hydroxyapatite 복합 필러의 피부 콜라겐 및 탄성섬유 재생효과를 조사하였다.

방법: 6주령 BALB/c 누드마우스 총 19마리를 정상피부, Radiesse, Restylane, HAc-nanoHAp, HAc-microHAp 5개 그룹으로 분류하였다. 필러를 주입 0,1,4,8,12주 후 필러의 부피를 평가 하기 위해 MRI 분석을 시행하였다. 그 외 조직학적 검사를 시행하는데, H&E stain을 하여 표피, 진피층의 두께변화와 섬유아세포의 증식을 보았고, Masson trichrome stain을 하여 콜라겐(collagen)의 양적인 변화를 측정하였고 Verhoeff-Van Gieson stain을 하여 탄성섬유(elastic fiber)의 양적인 변화를 측정하였다. Western blot 분석으로 collagen type 1, TGF-β1, Phosphorylated MAPK(Erk1/2), MAPK(Erk1/2), EGFR, Smad2/3 을 측정하였고, RT-PCR을 사용하여 type 1 procollagen, 모탄력소 (tropoelastin), fibrillin-1, EGFR, Smad2, Smad3 mRNA를 측정하였으며, 면역조직화학검사로 진피층의 모탄력소 (tropoelastin), vimentin을 측정하였다. 12주 후 나노입자 안전성을 평가 하기 위해 간, 폐, 비장, 신장 의 H&E stain을 시행 하였다.

결과: HAc-nanoHAp 그룹과 HAc-microHAp 그룹이 래디어스 와 레스텔렌 보다 모두에서 콜라겐 및 탄성섬유 생성이 더 많이 촉진 되고 필러의 지속성도 더 많이 촉진 되었다. 히알루론산의 콜라겐 및 탄성섬유 생성기전은 TGF-ß/Smad pathway 통과 한다고 확인하였다. 나노파티클의 독성 평가도 독성이 없는 것으로 판독을 받았다.

결론: HAc-nanoHAp과 HAc-microHAp 차이가 있지만, 콜라겐 및 탄성섬유 생성이 촉진 하는 것을 확인 하였다. 향후 광노화 동물 모델에서 이 복합 필러 의 피부주름 치료효과와 탄력성개선 효과를 평가해보겠다.

주요어: 탄성섬유, 콜라겐, 히알루론산, 하이드록시아파타이트, 히알루론산-하이드록시아파타이트 복합제, 필러, 래디어스, 레스텔렌

학 번: 2014-30869